Journal of Neurochemistry

JOURNAL OF NEUROCHEMISTRY | 2010 | 115 | 385–398 doi: 10.1111/j.1471-4159.2010.06933.x

The Reck tumor suppressor protein alleviates tissue damage and promotes functional recovery after transient cerebral ischemia in mice

Huan Wang,*[,1] Yukio Imamura,*[,1] Ryota Ishibashi,† Ediriweera P. S. Chandana,* Mako Yamamoto* and Makoto Noda*

*Department of Molecular Oncology, Kyoto University Graduate School of Medicine, Yoshida-Konoe-cho, Sakyo-ku, Kyoto, Japan

†Department of Neurosurgery, Kyoto University Graduate School of Medicine, Yoshida-Konoe-cho, Sakyo-ku, Kyoto, Japan

Abstract

The extracellular matrix (ECM) is important for both structural integrity and functions of the brain. Matrix metalloproteinases (MMPs) play major roles in ECM-remodeling under both physiological and pathological conditions. Reversion-inducing cysteine-rich protein with Kazal motifs (Reck) is a membrane-anchored MMP-regulator implicated in coordinated regulation of pericellular proteolysis. Although patho-physiological importance of MMPs and another group of MMP-regulators, tissue inhibitor of metalloproteinases, in brain ischemia has been demonstrated, little is known about the role of Reck in this process. In this study, we found that Reck is up-regulated in hippocampus and penumbra of subventricular zone after transient cerebral ischemia in mice. Most of the Reck-positive cells found at day 2 after ischemia are positive for Nestin as well as Ki67 and localized to the CA2 region of the hippocampus. At day 7 after ischemia, the Reck-positive cells increased in number, extended processes, expressed the reactive astrocyte marker GFAP and the neuronal marker NF200, and were widely distributed in the hippocampus. In the mutant mice carrying single functional *Reck* allele (*Reck+/–*), tissue damage and cell death after cerebral ischemia were augmented, the recovery of long-term potentiation in the hippocampus was compromised, NR2C subunit of NMDA receptor was up-regulated, gelatinolytic activity of MMPs were up-regulated and laminin-immunoreactivity was reduced. Our data implicate Reck in protection of ECM/tissue integrity and promotion of functional recovery in the brain after transient cerebral ischemia.

Keywords: cerebral ischemia, hippocampus, laminin, long-term potentiation, neural precursor cells, Reck.

J. Neurochem. (2010) **115**, 385–398.

Stroke is caused by a shortage of blood supply into the brain tissues. Previous studies revealed multiple events and pathways involved in ischemic damage, including excitotoxicity, oxidative stress, and apoptosis (Lo *et al.* 2003). Importance of some proteases, such as matrix metalloproteinases (MMPs) and tissue plasminogen activator, in some down-stream events in this process, such as breakdown of blood-brain barrier, has also been demonstrated (Wang *et al.* 1998; Yong *et al.* 2001; Lo *et al.* 2003). Studies on empirically effective cerebro-protective treatments, such as preconditioning, hypothermia, and microcirculation-stimulating agents, led to the discovery of a wide range of molecular events potentially contributing to the protection of ischemic brain (Dirnagl *et al.* 2003; Lo *et al.* 2003; Gidday 2006); however, the cause-effect relationships and relative importance among these events remain to be clarified.

Received April 18, 2010; revised manuscript received July 2, 2010; accepted July 21, 2010.

Address correspondence and reprint requests to Dr Yukio Imamura and Dr Makoto Noda, Department of Molecular Oncology, Graduate School of Medicine, Kyoto University, Yoshida-Konoe-cho, Sakyo-Ku, Kyoto 606-8501, Japan. E-mail: yimamura-ns@umin.net and mnoda@virus.kyoto-u.ac.jp

[1]These authors contributed equally to this study.

Abbreviations used: CCAO, common carotid artery occlusion; DG, dentate gyrus; ECM, extracellular matrix; fEPSP, field excitatory post-synaptic potential; GFAP, Glial fibrillary acid protein; Is, ischemia; LTP, long-term potentiation; MCAO, middle cerebral artery occlusion; MMP, matrix metalloproteinase; NPC, neural precursor cell; PB, phosphate-buffer; RECK, reversion-inducing cysteine-rich protein with Kazal motifs; SDS, sodium dodecyl sulfate; SVZ, subventricular zone; TTC, 2,3,5-triphenyltetrazolium chloride; TUNEL, TdT-mediated dUTP-x nick end labeling; WT, wild-type.

Activity-dependent long-term potentiation (LTP) of neurotransmission underlies certain forms of learning and memory (Bliss and Collingridge 1993; Whitlock *et al.* 2006). LTP can also be induced by pathological stimuli such as anoxia in the ischemic brain (Crepel *et al.* 1993). LTP occurs after a short period (e.g., a few minutes) of energy deprivation (Hammond *et al.* 1994), a treatment which induces transient cerebral ischemia and triggers ischemic tolerance (i.e., a pre-conditioning stimulus for cerebral protection) (Gidday 2006). It has been suggested that the ischemia-induced LTP plays a part in ischemic tolerance and post-ischemia recovery (Calabresi *et al.* 2003; Zhao *et al.* 2006; Ethell and Ethell 2007). More prolonged energy failure, on the other hand, is known to disrupt ionic homeostasis, leading to irreversible membrane depolarization and neuronal swelling (Calabresi *et al.* 1999, 2000; Centonze *et al.* 2001). The mechanisms underlying the recovery of LTP after such severe forms of ischemia remain unclear (Gillardon *et al.* 1999; Dirnagl *et al.* 2003), except that involvement of adult neurogenesis has been demonstrated (Nakatomi *et al.* 2002).

The extracellular matrix (ECM) is essential for animal development and homeostasis. MMPs are known to play major roles in ECM-degradation under physiological and pathological conditions (Sternlicht and Werb 2001). For instance, properly regulated MMP activities are essential for various events during CNS development, including cell proliferation, differentiation, migration, axonal growth, myelinogenesis, and angiogenesis (Yong *et al.* 2001; Wang *et al.* 2006). Importance of MMPs in CNS functions and synaptic plasticity has also been demonstrated (Meighan *et al.* 2006; Nagy *et al.* 2006; Ethell and Ethell 2007). On the other hand, MMPs may have detrimental effects on the structure and function of the brain in various diseases such as tumor invasion and metastasis, blood-brain barrier breakdown after stroke, and the inflammation, demyelination, and neuronal death associated with various neurological disorders (Sternlicht and Werb 2001; Yong *et al.* 2001). The sources of MMPs up-regulated after CNS injury and ischemia involve infiltrating leukocytes and intrinsic CNS cells (Ihara *et al.* 2001; Yong *et al.* 2001; Nakaji *et al.* 2006). Although the up-regulated MMPs have been implicated mainly in tissue damage, they may also contribute, when properly controlled, to the tissue repair and the restoration of neural functions (Wang *et al.* 2006).

Reversion-inducing cysteine-rich protein with Kazal motifs (Reck) was first isolated as a transformation suppressor gene by cDNA expression cloning (Takahashi *et al.* 1998). The *Reck* gene encodes a membrane-anchored MMP regulator essential for tissue integrity and angiogenesis during mammalian development (Oh *et al.* 2001; Noda and Takahashi 2007). Reck is expressed in Nestin-positive neural precursor cells (NPC) in developing CNS and supports NPC-proliferation by protecting Notch ligands (Muraguchi *et al.* 2007). Interestingly, coincidence of Nestin and Reck has also been found in developing neuromuscular junctions (Kawashima *et al.* 2008). RECK expression is altered under some pathological conditions including cancer (Noda *et al.* 2003; Noda and Takahashi 2007), rheumatoid arthritis (van Lent *et al.* 2005), osteoarthritis (Kimura *et al.* 2010) and cocaine abuse (Mash *et al.* 2007). Functions of Reck in adult brain, however, remain poorly understood.

In the present study, we examined the expression of Reck and the effects of reduced Reck expression after transient cerebral ischemia. Our data indicate that Reck is up-regulated in Nestin-positive cells in the hippocampus and contributes to the suppression of tissue damage and the recovery of LTP after ischemia.

Materials and methods

Preparation of ischemic mice

This study has been approved by Animal Research Committee, Kyoto University. The generation, PCR-based genotyping, and phenotypes of the *Reck*-null mice have been described elsewhere (Oh *et al.* 2001). The wild type (*wt*) and *Reck*-null heterozygous (*Reck*+/−) mice had the C57/BL6/J genetic background. All experiments were performed with the genotype in a blind manner. Male mice at 8 weeks old were deeply anesthetized by intraperitoneal injection of pentobarbital (45 mg/kg) or by exposing the animals to the 30% oxygen–70% nitrous oxide atmosphere containing 3% halothane as described by Kawashima *et al.* (2008). Mice were kept between a homeothermic blanket to keep the rectal temperature at 37.0 ± 1°C throughout the operation. For inducing brain ischemia, two protocols were employed: (i) bilateral common carotid artery occlusion (CCAO) for 1 h followed by reperfusion (Yang *et al.* 1997) which induces relatively mild ischemia in the whole brain, (ii) unilateral, intraluminal middle cerebral artery occlusion (MCAO) using a 8.0 siliconized filament for 25 min followed by reperfusion. We adapted the method of Nishimura *et al.* (2008) which induces severer ischemia confined in one hemisphere. Laser doppler flowmetry was used to confirm induction of ischemia and reperfusion. Only the mice that showed flow rate less than 1/10 after MCAO (i.e., typically ∼ 55 before ischemia and ∼ 5 after ischemia) were subjected to analyses. Cerebral infarct size was determined by staining 1-mm thick brain sections with 2,3,5-triphenyltetrazolium chloride (TTC, Sigma, St Louis, MO, USA). The area of infarction was quantified in digitized images of the section using the Image-J software (NIH, Bethesda, MD, USA). To exclude the effect of tissue swelling or edema, the infract size was calculated using the following formula (Lin *et al.* 1993): (area of contralateral hemisphere) – (area of undamaged ipsilateral hemisphere) [mm^2].

Immunohistochemical staining

Brain tissues were fixed in 1% *p*-formaldehyde in 0.1 M phosphate-buffer (PB, pH = 7.2). Frozen sections (10-μm thickness: coronal or sagittal sections) were prepared following the

method of Kawashima *et al.* (2008). Two types of staining were performed: (i) diaminobenzidine staining: non-specific signals were first blocked in 0.3% H_2O_2 in PB for 20 min at 25°C, and then Reck signals were detected using monoclonal anti-Reck antibody (see below), Envision+ kit (DAKO, Carpinteria, CA, USA), and diaminobenzidine visualization system, followed by counter-staining with Hematoxylin; (ii) Immunofluorescence staining: sections were first incubated in blocking solution containing 30% M.O.M. IgG blocking reagent (DAKO), 3% bovine serum albumin (SIGMA), 5% goat serum (DAKO), 0.5% Triton X-100, and 0.05% sodium azide for 60 min at 25°C, and then treated with primary antibodies, and finally with fluorescently labeled secondary antibodies (each incubation at 4°C overnight) diluted in the dilution buffer containing 3% bovine serum albumin, 5% goat serum, 0.5% Triton X-100, and 0.05% sodium azide. Slides were washed with PB saline for 5 min, three times at each step. Slides were mounted with Vectashield Mounting Medium containing 4′, 6-diamidino-2-phenylindole (Vector Laboratories, Burlingame, CA, USA). The primary antibodies used were anti-Reck (5B11D12, mouse monoclonal; Takahashi *et al.* (1998), anti-IBA1 (rabbit polyclonal; WAKO, Osaka, Japan), anti-Nestin (rabbit polyclonal; Santa Cruz Biotechnology, Santa Cruz, CA, USA, mouse monoclonal; Chemicon, Temecula, CA, USA), anti-Ki67 (rabbit polyclonal; Novocastra, Wetzlar, Germany), anti-neurofilament 200 (rabbit polyclonal; SIGMA), anti-laminin (mouse monoclonal; SIGMA), anti-CD31 (rabbit polyclonal; BD Transduction Laboratories, Lexington, KY, USA), anti-Glial fibrillary acid protein (GFAP) (rabbit polyclonal; DAKO) and anti-NR2C (rabbit polyclonal; phosphosolutions). The secondary antibodies used were Alexa Fluor 488 goat anti-mouse IgG (Invitrogen, Carlsbad, CA, USA) for monoclonal Reck and anti-laminin and Alexa Fluor 555 goat anti-rabbit IgG (Invitrogen) for the other primary antibodies raised in the rabbit. The images were recorded using a fluorescent microscope (Zeiss, Tokyo, Japan) and/or a confocal laser scanning microscope (Olympus, Tokyo, Japan). The number of immunoreactive cells on each slice was determined using the Image-J software. Statistical significance of difference was assessed by Student's *t*-test.

TUNEL assay

TdT-mediated dUTP-x nick end labeling (TUNEL) assay was performed using the In Situ Cell Death Detection Kit (Roche Molecular Biochemicals, Indianapolis, IN, USA) following the manufacturer's protocol. Frozen sections (10-μm thick) from wild-type (WT) or Reck+/− mice were post-fixed with 4% *p*-formaldehyde at 25°C for 20 min and then incubated in 0.1% citric acid solution containing 0.1% Triton X-100 at 37°C for 30 min for permeabilization. The slices were incubated in the mixture of 90% Label Solution and 10% Enzyme Solution at 37°C for 90 min and mounted with the solution containing 4′, 6-diamidino-2-phenylindole (Vector). TUNEL-positive cells in the hippocampus were recorded with a confocal laser scanning microscope and counted using the Image-J software.

Immunoblot assay

Tissues samples of cerebral cortex, hippocampus, and brainstem were collected from WT or Reck+/− mice at 7 days after ischemia, and homogenized in the lysis buffer containing 50 mM Tris–HCl (pH 7.5), 150 mM NaCl, 1% Triton X-100, 10% glycerol, 0.5% sodium dodecyl sulfate (SDS), 1.5 mM $MgCl_2$, 1 mM EDTA and the protease inhibitor cocktail (03969-21, Nacalai tesque, Kyoto, Japan). The amount of protein in each sample was determined by standard bicinchoninic acid assay (Thermo Scientific, Waltham, MA, USA). The proteins were separated by SDS–polyacrylamide gel electrophoresis and analyzed by immunoblot assay as described previously (Muraguchi *et al.* 2007).

Slice culture and gelatin zymography

Organotypic slice culture described previously (Stoppini *et al.* 1991; Imamura *et al.* 2003) was adapted to gelatin zymography. In brief, eight pieces of hippocampal slices (300-μm thick) were placed submerged in Dulbecco modified eagle medium onto the culture plate inserts (Millicell-CM, 0.4 μm, 30 mm diameter, Millipore Corporation, Bedford, MA, USA) set in 6-well culture plates and incubated for 24 h. The medium in the lower compartment (800 μL) were collected and analyzed by gelatin zymography as described previously (Oh *et al.* 2001), using SDS–polyacrylamide gel electrophoresis (10% polyacrylamide containing 1 mg/mL gelatin). The amount of sample loaded was normalized against the amount of tissue per well, as estimated by bicinchoninic acid assay of tissue lysate.

RNA extraction and analyses

Total RNA was extracted using NucleoSpin RNAII (Macherey-Nagel, Düren, Germany) and subjected to quantitative RT-PCR using SuperScriptIII Platinum (SYBR Green) one-step quantitative RT-PCR kit (Invitrogen, Carlsbad, CA, USA) and the Mx3005P QPCR system (Stratagene, La Jolla, CA, USA). Gapdh was used as an internal control. The sequences of the primer sets (F, forward; R, reverse) and the probe used were as follows: Reck-F: 5′-aggtctccagcagtctcc, Reck-R: 5′-gcagttccttccagttgtg, Reck Molecular Beacon probe: 5′FAM-cgcgatcccactccctgcctcctcctcagatcgcg-Eclipse, Gapdh-F: 5′-tcaacggcacagtcaagg, and Gapdh-R: actccacgacatactcagc. Reaction conditions: 50°C, 5 min; 95°C, 5 min; followed by 45 cycles of 94°C, 5 min; 55°C, 40 s; 72°C, 15 s.

Electrophysiological recording

Electrophysiological experiments were performed using multi-electrode array devices (MED64, α-MED Science, Osaka, Japan). We used this system to record the field excitatory post-synaptic potential (fEPSPs) for studying the propagation of synaptic transmission simultaneously from 64 points on a hippocampal slice. Acute hippocampal slices from WT and Reck+/− mice were prepared and maintained in perfusion (2–3 mL/min) of artificial CSF [NaCl (126), KCl (2.5), $MgCl_2$ (1), $NaHCO_3$ (26), NaH_2PO_4 (1.25), $CaCl_2$ (2) and D-glucose (10), components in mM, pH = 7.3] as described elsewhere (Imamura *et al.* 2008). We also used modified low-Mg^{2+} artificial CSF solution (MgCl: 0.1 mM) for the recording of LTP. Perforant path fibers in the dentate gyrus of hippocampal slices were stimulated in a test pulse of half maximum intensity with 30-s intervals. Following the test pulse recording for 10 min to confirm the stability of the baseline synaptic current amplitude, high frequency stimuli (four 1-s bursts at 100 Hz with 5-min intervals) (Nagy *et al.* 2006) were applied to induce LTP. Post-tetanic synaptic currents were recorded from all

the electrodes for 1 h, and the data were analyzed using the Mobius software (α-MED Science, Japan).

Results

Up-regulation of Reck in the hippocampus after transient cerebral ischemia

To obtain some clues to the functions of Reck in the adult brain, we monitored the level of Reck-immunoreactivity in the serial coronal sections of the brain (every 50 μm) prepared from mice after bilateral CCAO for 1 h followed by reperfusion. Seven days after ischemia ('Is 7d'), numerous strong Reck signals were found along striatum radiatum of the hippocampus (Fig. 1a, panel 2; magnified view in panel 3). At this time point, significant increase in the level of Reck protein in the hippocampus could be detected by immunoblot assay (Fig. 1b, lane 2 vs. 5). Increased in the level of *Reck* mRNA after ischemia was also detectable by quantitative qRT-PCR using the total hippocampal RNA (Fig. 1c). Hence, ischemia up-regulates Reck in the hippocampus at the mRNA level.

The number and distribution of Reck-positive cells after cerebral ischemia

To examine the properties and behaviors of the ischemia-induced Reck-positive cells, we performed mild ischemia (CCAO). At day 2 after CCAO, Reck-positive cells were found mainly in the CA2/CA3 region of the hippocampus (Fig. 2a, panel 1; Fig. 2b, bar 2). Interestingly, most of these cells are round in shape (Fig. 2a, panel 3). In contrast, at day

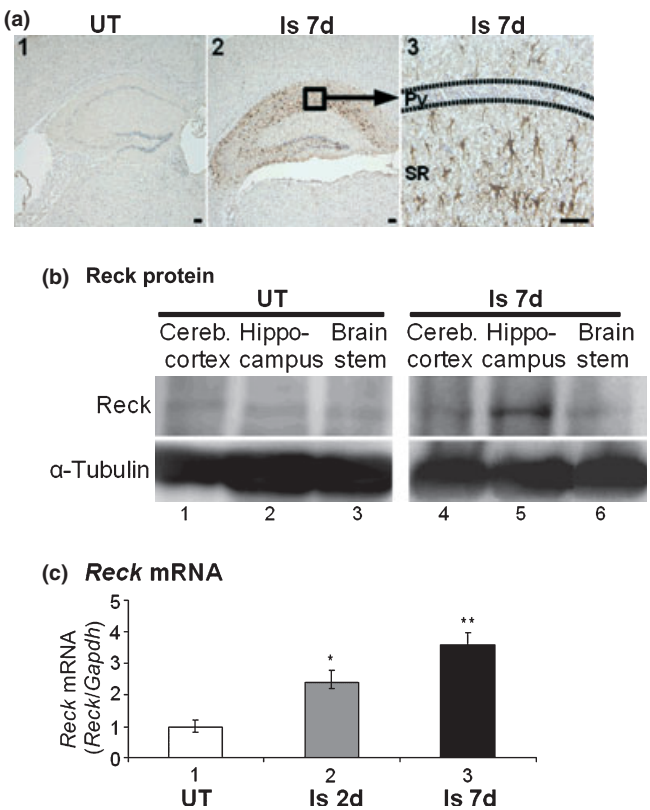

Fig. 1 Up-regulation of Reck after transient cerebral ischemia (CCAO). (a) Reck immunoreactivity at day 7 in a brain slice from an untreated mouse (UT; panel 1) or a mouse at day 7 after CCAO (Is 7d; panels 2 and 3). Coronal sections at 2 mm caudal from the bregma are shown. Py, pyramidal cell layer; SR, striatum radiatum. Scale bar: 50 μm. At this time point, numerous process-extending cells with strong Reck-immunoreactivity were found in the hippocampus (panel 2, low magnification), especially in the striatum radiatum (panel 3, higher magnification). (b) Up-regulation of Reck protein after CCAO. Lysates (100 μg) of indicated tissues from an untreated mouse (UT) or a mouse at day 7 after CCAO (Is 7d) were subjected to immunoblot assay. α-Tubulin was used as a loading control. Up-regulation of Reck protein in the hippocampus after ischemia was detectable (lane 5). (c) Up-regulation of *Reck* mRNA after CCAO. Total RNA (10.25 μg) isolated from the whole hippocampus of untreated mouse (UT), mouse at day 2 after ischemia (Is 2d), or at day 7 after ischemia (Is 7d) were subjected to qRT-PCR. The value for *Reck* normalized against the reference gene *Gapdh* was divided by the normalized value for the untreated animal. *Reck/Gapdh* (mean ± SEM): UT, 1.00 ± 0.18, $n = 6$; Is 2d, 2.39 ± 0.27, $n = 4$, *significantly different from UT ($p = 0.028$); Is 7d, 3.58 ± 0.33, $n = 5$, **significantly different from UT ($p = 0.005$).

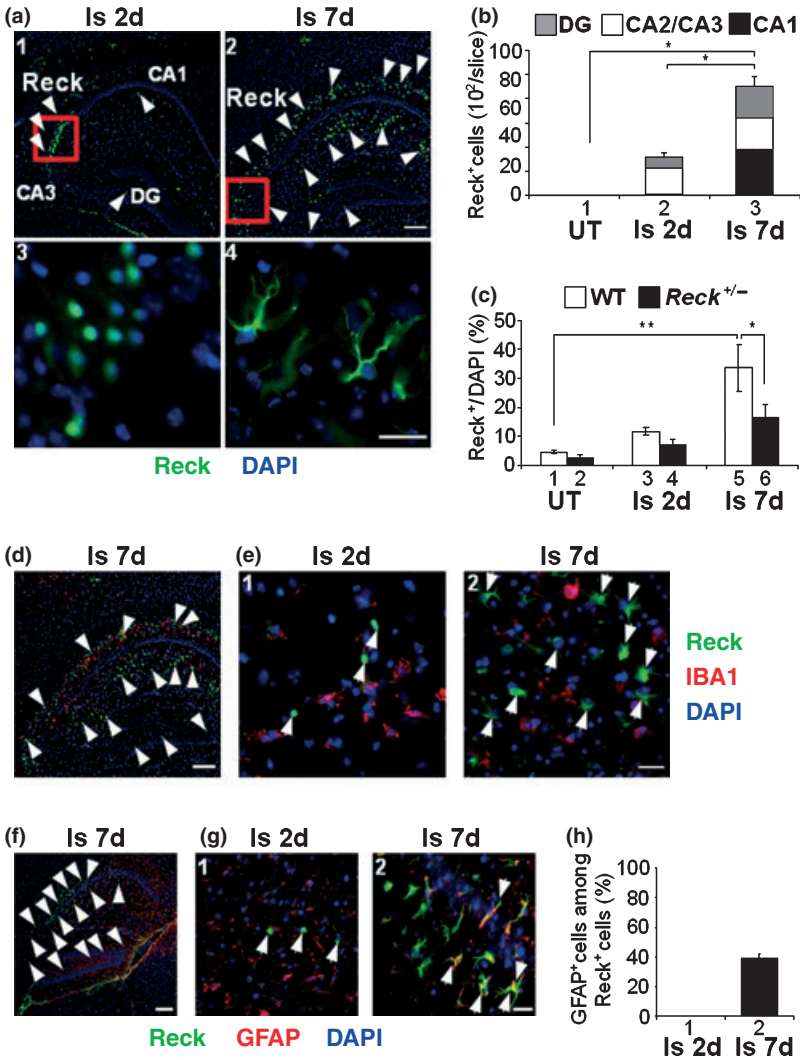

Fig. 2 Distribution of Reck-positive cells in the hippocampus of mice after CCAO. (a) Sagittal sections of the brain from wild type mice at day 2 (panels 1, 3) or day 7 (panels 2, 4) after CCAO were subjected to immunofluorescent staining with Reck (green) followed by nuclear counter-staining with DAPI (blue). Magnified views of the areas indicated by red squares in panels 1 and 2 are shown in panels 3 and 4, respectively. Scale bar: 200 μm (panels 1, 2), 20 μm (panels 3, 4). Some of the Reck-positive cells are indicated by arrowheads. Note the round Reck-positive cells found in the CA2/CA3 region of the hippocampus at day 2 (panels 1, 3) and the Reck-positive, process-extending cells found more widely and abundantly in the hippocampus at day 7 (panels 2, 4). (b) Temporal changes in the distribution of Reck-positive cells in the wild type mice after CCAO. Reck-positive cells in three hippocampal areas (i.e., DG, CA2/CA3, CA1) were scored separately. The whole bar represents the total number of Reck-positive cells, and the patterned sections (grey, DG; white, CA2/CA3; black, CA1) represent the numbers in individual areas (mean ± SEM; $n = 35–40$ slices from four animals). (c) Proportion of Reck-positive cells in the hippocampus of *WT* (white bar) or *Reck+/–* mice (black bar) left untreated (UT) or at day 2 (Is 2d) or day 7 (Is 7d) after CCAO. The ratio between the cells bearing detectable levels of Reck signals and the total number of DAPI spots (nuclei) found in the hippocampus was scored using immunofluorescent images as shown in (a). Bar represents mean ± SEM ($n = 40–45$ slices from four to six animals). $^{**}p < 0.01$, $^{*}p < 0.05$ (Student's *t*-test). (d, e) The Reck-positive cells do not coincide with IBA1-positive cells. Brain slices from wild type mice at day 2 (Is 2d) or day 7 (Is 7d) after CCAO were subjected to immunofluorescent double staining for Reck (green) and the microglial marker IBA1 (red). Some of the Reck-positive cells are indicated by arrowheads. Scale bar: 200 μm (d), 50 μm (e). (f, g) The Reck-positive cells do not coincide with GFAP-positive cells at day 2, but coincide at day 7. Brain slices from wild type mice at day 2 (Is 2d) or day 7 (Is 7d) after CCAO were subjected to immunofluorescent double staining for Reck (green) and the glial marker GFAP (red). Scale bar: 200 μm (f), 50 μm (g).

7, Reck-positive cells were found more widely and abundantly in all areas of the hippocampus (Fig. 2a, panel 2; Fig. 2b, bar 3). At this stage, Reck-signals are found in the cells extending prominent processes (Fig. 2a, panel 4).

Importantly, the number of Reck-positive cells, as scored under the same conditions, was significantly lower in Reck+/− mice than in WT mice (Fig. 2c).

Participation of the ischemia-induced Reck-positive cells to neuro-protection

Microglia is known to be abundant after cerebral ischemia in the hippocampus and striatum. The two areas are known to be highly vulnerable to cerebral ischemia (Pforte *et al.* 2005) and excitotoxicity (Koizumi *et al.* 2007). Double staining for Reck and a microglial marker (IBA1) demonstrated that although Reck-positive cells and microglia were abundant in the same areas after CCAO (Fig. 2d), the cells doubly positive for two markers were rare (< 4%; Fig. 2e), suggesting that the Reck-positive cells are different from microglia.

Inducible reactive astrocytes after cerebral ischemia are thought to determine neuro-protection (Li *et al.* 2008). We examined the double-staining of Reck-positive cells and reactive astrocyte marker (GFAP) -positive cells (Fig. 2f). We found 40% Reck-positive cells were GFAP-positive cells at day 7 after CCAO (Fig. 2g). These findings suggest that Reck participate in regeneration after cerebral ischemia.

Characterization of the ischemia-induced Reck-positive cells

To obtain some clues to the identity of these Reck-positive cells, we employed three additional markers: the proliferation marker Ki67, NPC marker Nestin, and neuronal marker NF200 (Fig. 3). First, we determined the numbers of Ki67-positive cells and Nestin-positive cells in the hippocampal slices before and after CCAO (Fig. 3a). A considerable number of Ki67-positive cells were present in untreated group (UT), especially in dentate gyrus (DG), and their number slightly increased at day 2 and slightly decreased at day 7 after CCAO (Fig. 3a, panel 1). In contrast, Nestin-positive cells were absent in untreated group, emerged at day 2 after CCAO, mainly in CA2/CA3, and became widely distributed, though decreased in total number, at day 7 (Fig. 3a, panel 2). The distribution of Nestin-positive cells at day 2 (Fig. 3a, panel 2, bar 2) is reminiscent of that of Reck-positive cells (see Fig. 2b, bar 2). Proportion of Ki67-positive cells among the Nestin-positive cells was relatively high (∼ 70%) at day 2 and decreased (∼ 35%) at day 7 (Fig. 3a, panel 3), while proportion of Nestin-positive cells among the Ki67-positive cells stayed relatively low (< 25%) at both time points (Fig. 3a, panel 4). These findings indicate that the Nestin-positive cells that emerged at day 2 in CA2/CA3 (Fig. 3a, panel 2, bar 2) were largely proliferative (Fig. 3a, panel 3, bar 1) and most likely represented NPCs, whereas the Ki67-positive cells included both NPCs and other types of cells (Fig. 3a, panel 4, bar 1) that were proliferative even in untreated animals (Fig. 3a, panel 1, bar 1). At day 7, proliferative potential of Nestin-positive cells declined (Fig. 3a, panel 3, bar 2).

Next, we analyzed the relationships between these two markers and Reck (Fig. 3b and c). At day 2, large fractions of Reck-positive cells were Ki67-positive (> 70%; Fig. 3b, panel 3, bar 1) and Nestin-positive (∼ 90%; Fig. 3c, panel 3, bar 1). Importantly, a large fraction of Nestin-positive cells were Reck-positive (> 90%; Fig. 3c, panel 4, bar 1), while only a part of the Ki67-positive cells were Reck-positive (< 40%; Fig. 3b, panel 4, bar 1) at day 2, indicating that the Reck-positive population and Nestin-positive population were largely overlapped while the Ki67-positive population included a large population of Reck-negative cells (Fig. 3e, upper panel). At day 7, proliferative potential of the Reck-positive cells (Fig. 3b, panel 3, bar 2) and the overlap between Reck-positive and Nestin-positive populations decreased (Fig. 3c, panels 3 and 4, bar 2). Hence, a large fraction of the Reck-positive cells had a character of NPCs (i.e., Ki67/Nestin-double positive) at day 2, but the proportion of such cells among the Reck-positive cells declined at day 7. The reduction of Ki67-positive cell (Figure S1a) and Nestin-positive cell (Figure S1b) in *Reck*+/− mice confirm the relevance of Reck for neural precursor cell expression.

Finally, we examined the relationship between NF200 and Reck (Fig. 3d). Although the proportion of NF200-positive cells among the Reck-positive cells was small at day 2 (∼ 15%; Fig. 3d, panel 3, bars 1–3), it increased dramatically at day 7 in all areas of the hippocampus (∼ 70%; Fig. 3d, panel 3, bars 4–6). Taken together, these data indicate that the Reck-positive cells found in CA2/CA3 on day 2 have a character of NPCs while those found widely in the hippocampus at day 7 have a character of neurons (Fig. 3e).

Reck is required for the recovery of LTP in the hippocampus after ischemia

To better understand the functions of the Reck-positive cells found after ischemia in the hippocampus, we used multi-electrode plates to record fEPSP in the hippocampal slices prepared from un-operated mice or from mice after CCAO (Fig. 4). Test pulse stimulations (0.033 Hz, 30-s interval) were applied at perforant path fibers in DG (white arrow in Fig. 4a), and the inward fEPSP was recorded at various hippocampal areas.

In control experiments using un-operated *WT* mice, the inward fEPSP from all recording electrodes were abolished after addition of tetrodotoxin (1 μM in Fig. 4b), indicating that the signals were mainly evoked by the activation of neuronal synaptic transmission. After high-frequently stimulations (100 Hz, 1 s, four times with 5-min intervals), these slices showed robust LTP (180.2 ± 2.5%, $n = 5$) (Fig. 4c). When similar experiments were performed using slices prepared from *WT* mice at day 2 after CCAO, the success

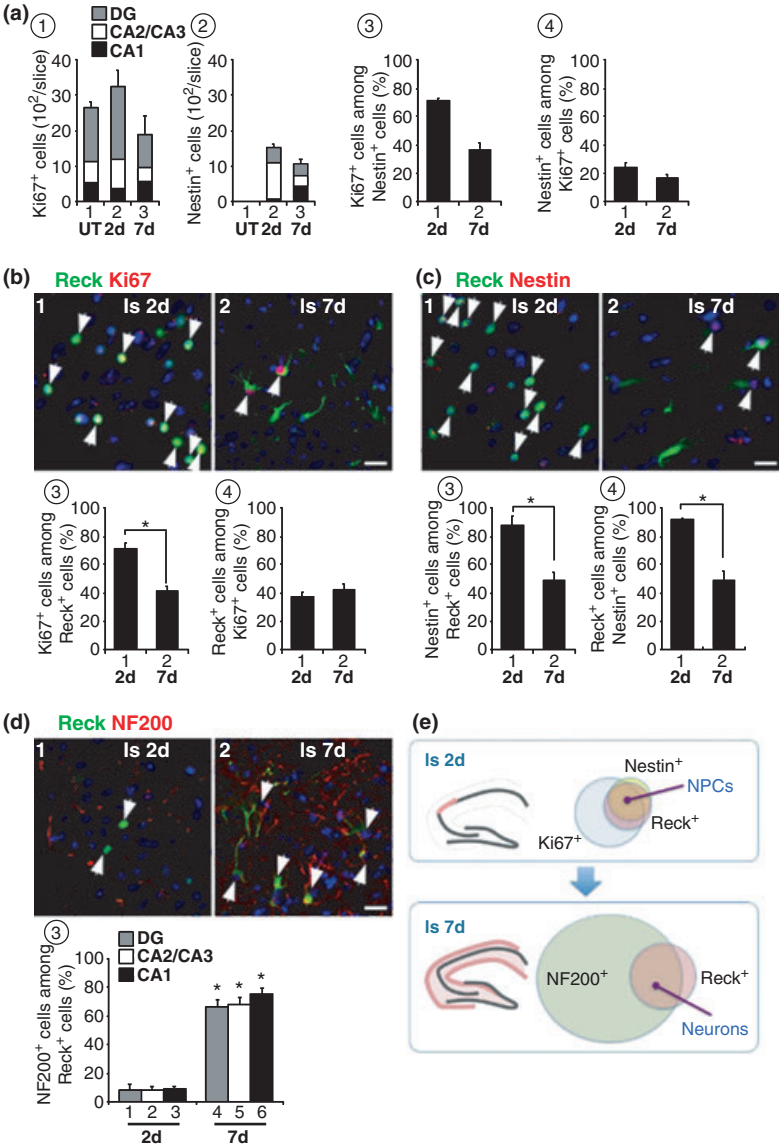

Fig. 3 Properties of ischemia-induced Reck-positive cells. (a) Relationship between Ki67-positive cells and Nestin-positive cells found in the hippocampus. Sagittal brain sections from untreated wild type mice (UT) or the mice at day 2 (2d) or day 7 (7d) after CCAO were subjected to immunofluorescent double staining for Ki67 and Nestin. Panel 1: The number of Ki67-positive cells in three hippocampal areas. Panel 2: The number of Nestin-positive cells in three hippocampal areas. In these two panels, the whole bar represents the total number, and its compartments (grey, DG; white, CA2/CA3; black, CA1) the numbers in respective areas (mean ± SEM; $n = 55$–60 slices from four to six animals). Panel 3: Proportion of Ki67-positive cells among Nestin-positive cells. Panel 4: Proportion of Nestin-positive cells among Ki67-positive cells. (b) Relationship between Reck-positive cells and Ki67-positive cells found in the hippocampus. Sagittal brain sections from wild type mice at day 2 (panel 1) or day 7 (panel 2) after CCAO were subjected to immunofluorescent double staining for Reck (green) and Ki67 (red). Panel 3: Proportion of Ki67-positive cells among Reck-positive cells. Panel 4: Proportion of Reck-positive cells among Ki67-positive cells. In panels 3 and 4, bar represents mean ± SEM, $^*p < 0.05$ (Student's *t*-test). (c) Relationship between Reck-positive cells and Nestin-positive cells found in the hippocampus. Sagittal brain sections from wild type mice at day 2 (panel 1) or day 7 (panel 2) after CCAO were subjected to immunofluorescent double staining for Reck (green) and Nestin (red). Panel 3: Proportion of Nestin-positive cells among Reck-positive cells. Panel 4: Proportion of Reck-positive cells among Nestin-positive cells. In panels 3 and 4, bar represents mean ± SEM, $^*p < 0.05$ (Student's *t*-test). (d) Relationship between Reck-positive cells and NF200-positive cells found in the hippocampus. Sagittal sections of the brains were doubly stained for Reck (green) and NF200 (red). Panel 3: Proportion of NF200-positive cells among Reck-positive cells in respective areas. Bar represents mean ± SEM, $^*p < 0.05$ (Student's *t*-test). In (b–d), arrowheads indicate the round Reck-positive cells in panel 1 and the process-extending cells in panel 2. Scale bar: 50 μm. (e) Summary of the findings.

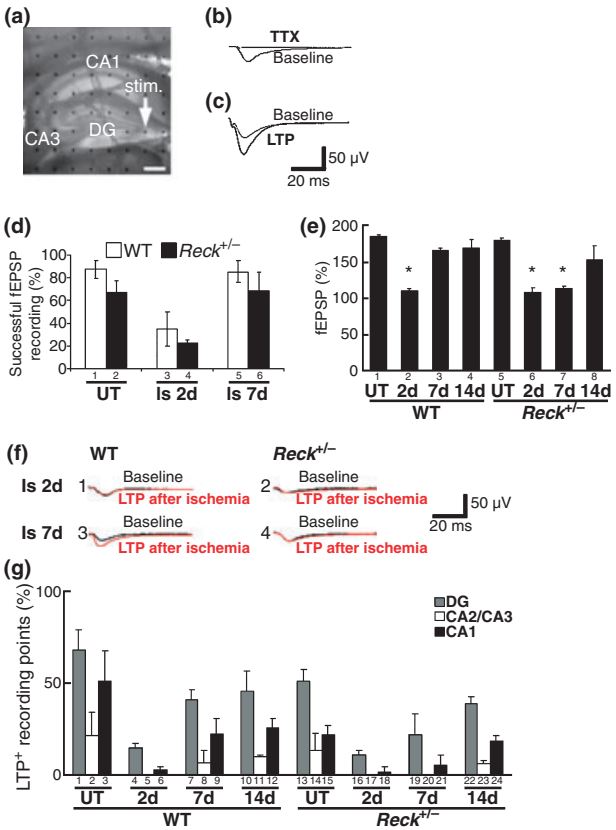

Fig. 4 Reck is necessary for recovery of hippocampal LTP after CCAO. (a–c) Control experiments with hippocampal slices from untreated wild type mice. (a) An acute hippocampal slice placed on a 8 × 8 multi-electrode dish (MED probe). The distance between adjacent electrodes (dark dots) is 300 μm. Electrical stimulation with half-maximum intensity (white arrow: stimulation, 30-s interval, 200-μs duration) was applied to the perforant path fibers of DG (marked 'stim.'), and the evoked field excitatory post-synaptic potentials (fEPSP) were recorded from all the other electrodes covered by the hippocampus. (b) A typical trace of evoked potential (thick trace) which was abolished after application of tetradotoxin (1 μM; thin trace). (c) Typical traces before (thin trace) and after (thick trace) the hippocampal LTP induced by a burst of high frequency stimulation at the same electrode. (d–g) Comparison between *WT* and *Reck+/–* mice left untreated (UT) or at day 2 (Is 2d) or day 7 (Is 7d) after CCAO. (d) Success rate of fEPSP recording. Proportion of the slices giving rise to fEPSP signals among all the slices tested from each group are shown. Bar represents mean ± SEM (%); $n = 14$ slices from four animals. (e) Loss and recovery of LTP after CCAO. Bar represents the extent of LTP [mean ± SEM (%); $n = 14$ slices from four animals] after the high frequency stimulation among the slices which gave rise to successful fEPSP recording, as shown in (d). *Significantly different from UT ($p < 0.05$, Student's *t*-test). (f) Typical traces before (black) and after (red) high frequency stimulation. (g) Proportions of the recording points that gave rise to successful LTP. Bar represents mean ± SEM of the proportion of recording points that gave rise to LTP (> 150%) among the recording points that gave rise to successful fEPSP recording in respective areas of the hippocampus ($n = 12–16$ slices from four animals).

rate of inward fEPSP-recording decreased (Fig. 4d, bar 3), and even in successful cases, LTP was barely detectable (Fig. 4e, bar 2; Fig. 4f, trace 1; Fig. 4g, bars 4–6). At day 7, however, both inward fEPSP (Fig. 4d, bar 6) and LTP (Fig. 4e, bar 3; Fig. 4f, trace 3; Fig. 4g, bars 7–9) were again detectable, suggesting functional recovery.

In *Reck+/–* slices, success rates of inward fEPSP-recording at different time points showed a profile similar to that in *WT* slices, although the values were slightly lower as compared to *WT* slices (Fig. 4d, bars 2, 4, 6). Nevertheless, these data indicate that the neuronal activity itself was restored to the original level by day 7 after CCAO in *Reck+/–* mice. Importantly, however, LTP remained barely detectable at day 7 in *Reck+/–* mice (Fig. 4e, bar 6; Fig. 4f, trace 4) but detectable at day 14 (Fig. 4e, bar 8). The recovery is particularly compromised in CA2/CA3 and CA1 (Fig. 4g, bars 8, 9 vs. bars 17, 18). These data indicate the delayed recovery of the hippocampus for synaptic plasticity after cerebral ischemia in *Reck+/–* mice.

Increased glutamate receptor NR2C subunit expression in *Reck+/–* mice

NR2C subunit of NMDA glutamate receptor is augmented after ischemic events (Small *et al.* 1997) or hypoxia (Bickler *et al.* 2003) and mainly contributes to the glutamate excitotoxicity (Kadotani *et al.* 1998). NR2C-immunoreactivity was determined by immunofluorescent staining of untreated slices observed under the same exposure of microscopy (Fig. 5a). NR2C-immunoreactivity in the hippocampus in *Reck+/–* mice was significantly higher than WT mice (Fig. 5b; $p < 0.05$) and NR2C subunit expression was also up-regulated (Fig. 5c).

These results suggest that Reck has an activity to reduce tissue damage via inhibition of glutamate excitotoxicity after cerebral ischemia.

Reck protects laminin after CCAO

Next, we analyzed the status of ECM in the hippocampus before and after CCAO. Among the ECM components, laminin is of particular interest, as previous paper reports its activity to support hippocampal LTP after ECM degradation (Nakagami *et al.* 2000). Immunofluorescent staining indicate that laminin-immunoreactivity was more abundant in *WT* hippocampus than in *Reck+/–* hippocampus before ischemia (Fig. 6a, panel 1 vs. 7; Fig. 6b, bars 1, 2). At day 2 after CCAO, laminin signals decreased in both *WT* and *Reck+/–* mice, and the difference between the two groups became marginal (Fig. 6b, bars 3, 4). Importantly, at day 7 after CCAO, laminin-signals increased in *WT* mice but not in *Reck+/–* mice (Fig. 6b, bars 5, 6). Double staining indicated that these laminin-signals were mainly associated with CD31-positive vascular endothelial cells (Fig. 6c) and not with NF200-positive neurons (Fig. 6d). These results indicate that Reck not only elevate the steady state level of

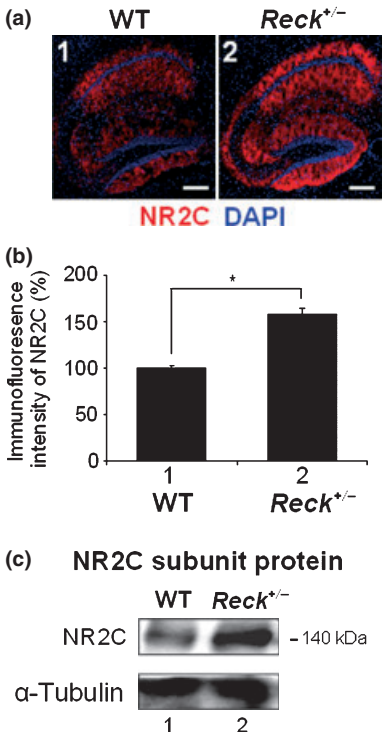

Fig. 5 NR2C subunit up-regulation in hippocampal slices of *Reck+/–* mice. (a) Immunoreactivity of NR2C subunit in WT and *Reck+/–* mice. Scale bar: 100 μm. (b) NR2C immunoreactivity enhancement in *Reck+/–* mice. Bar represents mean ± SEM; (n = 40–60 slices from five animals). *p < 0.05 (Student's t-test). (c) Expression of NR2C subunit protein in untreated WT or *Reck+/–* mice. Lysates (200 μg) from indicated tissues were subjected to immunoblot assay. α-Tubulin was used as a loading control (n = 5–7 animals).

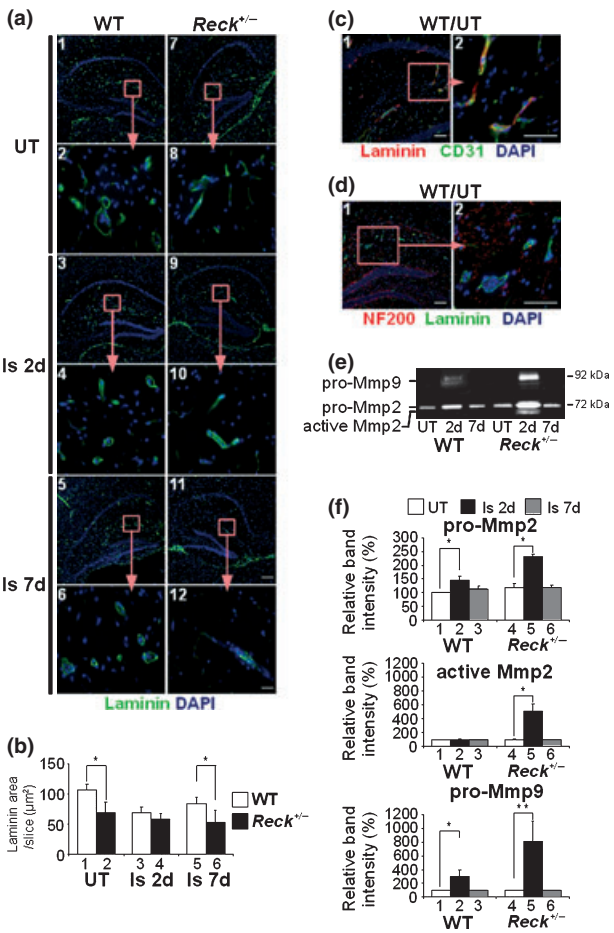

Fig. 6 Reck protect Laminin degraded by gelatinases after CCAO. (a) Sagittal brain sections from untreated (UT) wild type (WT) or *Reck+/–* mice or the mice at day 2 (Is 2d) or day 7 (Is 7d) after CCAO were subjected to immunofluorescent staining for laminin (green) followed by nuclear counter-staining with DAPI (blue). Magnified view of the area indicated by red box in the upper panel is shown in the lower panel. Scale bar: 200 μm (upper panel), 20 μm (lower panel). (b) Quantification of laminin-immunoreactivity. On laminin-immunofluorescence images recorded under the same conditions, the areas in which fluorescence intensity exceeds a threshold level were measured using the Image J software. The value relative to that of untreated WT mice is presented. Bar represents mean ± SEM. (c) Relationship between laminin and CD31-positive cells in the hippocampus of untreated wild type mouse. Scale bar: 100 μm. (d) Relationship between laminin and NF200-positive cells in the hippocampus of untreated wild type mouse. Scale bar: 100 μm. (e) Gelatin zymography of the proteins released from cultured hippocampal slices of *WT* or *Reck+/–* mice left untreated (UT) or at day 2 (2d) or day 7 (7d) after CCAO. Positions of the pro-Mmp-2 (72 kDa), active Mmp-2 and pro-Mmp-9 (92 kDa) bands are indicated. (f) Densitometric quantification of gelatinase bands. Pro-Mmp-2, active Mmp-2 and Mmp-9 are up-regulated at day 2 after CCAO and returned to the basal levels at day 7. Bar represents mean ± SEM (n = 5 animals). **p < 0.01, *p < 0.05 (Student's t-test).

laminin associated with hippocampal vasculature (i.e., vascular basal lamina) but also supports the recovery of the laminin reduced after ischemia.

Finally, we performed gelatin zymography to determine the level of gelatinases (pro-Mmp-2, active MMP-2 and pro-Mmp-9) known to be up-regulated after acute cerebral ischemia (Gu *et al.* 2002; Tsuji *et al.* 2005; Rosell *et al.* 2006; Fujimoto *et al.* 2008) or chronic hypoperfusion (Nakaji *et al.* 2006). We found that pro-MMP-2 (72 kDa), active Mmp-2 and pro-MMP-9 (92 kDa) were up-regulated at Is 2d in WT and *Reck+/–* mice (Fig. 6e and f). Importantly, at Is 2d, MMP-2 and MMP-9 expression was significantly higher in the *Reck+/–* mice, suggesting the higher MMP-dependent degradation of ECM in the *Reck+/–* mice. Hence, reduced laminin in *Reck+/–* mice can be explained by up-regulated gelatinase expression.

Increased ischemic damage in *Reck+/–* mice

To test whether MMPs gelatinolytic activity between these mice causes any difference in response to brain ischemia, we

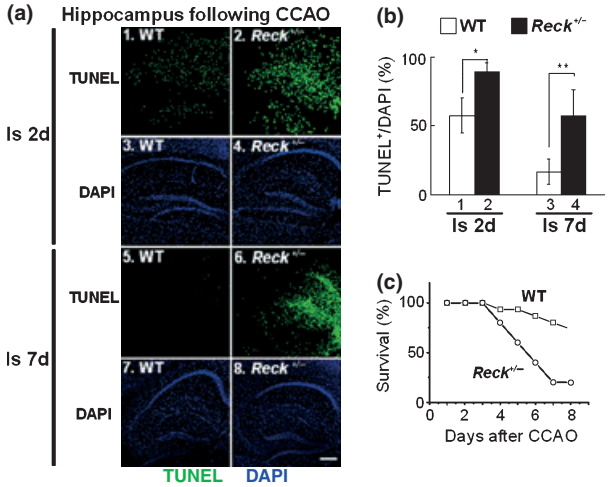

Fig. 7 Reck reduces ischemic cell death after CCAO. (a) Sagittal brain sections from *WT* (left panels) and *Reck+/–* mice (right panels) at day 2 (Is 2d) or day 7 (Is 7d) after CCAO were subjected to *in situ* TUNEL assay to assess the extent of apoptotic cell death. Corresponding DAPI image (i.e., nuclei) (panels 3, 4, 7, 8) are shown below each TUNEL image (panels 1, 2, 5, 6). Scale bar: 200 μm. (b) Proportion of TUNEL-positive cells and the nuclei in the images as shown in (a). Bar represents mean ± SEM (n = 35–40 slices from three to four animals). (c) Survival curves of the *WT* and *Reck+/–* mice after CCAO. At day 7: *WT*, 73.3% (n = 16), *Reck+/–*, 18.2% (n = 11). *; $p < 0.05$, **; $p < 0.01$.

prepared hippocampal slices from mice at day 2 or day 7 after CCAO, and performed *in situ* TUNEL assay. Interestingly, the TUNEL-positive (i.e., apoptotic) cells were more abundant in *Reck+/–* mice than in *WT* mice (Fig. 7a and b). Moreover, the number of apoptotic cells seems to decrease more rapidly in *WT* mice than in *Reck+/–* mice (Fig. 7b; bar 1 vs. 3, bar 2 vs. 4). Survival curves of the animals after CCAO (Fig. 7c) indicate lower tolerance of *Reck+/–* mice to the cerebral ischemia.

Finally, we performed unilateral, transient MCAO (25 min) and examined its effects by preparing brain slices (1-mm thick) after 24 h, followed by staining with TTC. TTC stains the cells with intact mitochondrial activity in red, leaving dead cells unstained (Fig. 8). The lesions of infarction (white areas) were significantly larger in *Reck+/–* mice than in *WT* mice (Fig. 8a and b; $p < 0.01$). Double-staining of Reck and progenitor markers indicated that Reck is found in nestin-positive cells (Fig. 8e, panel 1; Fig. 8f, bar 1), Ki67-positive cells (Fig. 8e, panel 2; Fig. 8f, bar 2) but rare in GFAP-positive cells (Fig. 8e, panel 3; Fig. 8f, bar 3) in the subventricular zone of the striatum (SVZ). These findings, using MCAO, are consistent to our model that Reck support neuroprotection and followed by neurogenesis after cerebral ischemia.

Discussion

In this study, we found that at day 1 after severe form of cerebral ischemia (MCAO), Reck was found in Ki67- and Nestin-positive cells from penumbra and SVZ, on the other hand, at day 2 after a relatively mild form of cerebral ischemia (CCAO), some round cells positive for Reck, Ki67, and Nestin emerge in the CA2/CA3 region of the hippocampus and that at day 7, numerous process-extending cells positive for Reck and NF200 are present more widely in the hippocampus. Previous studies indicate that ischemia induces adult neurogenesis in some areas such as SVZ and DG in the hippocampus (Nakatomi *et al.* 2002; Ernst and Christie 2005; Namba *et al.* 2005; Felling *et al.* 2006). The round Reck-positive cells found in the CA2/CA3 region have some characters of NPCs and may therefore represent a previously unappreciated form of ischemia-induced adult neurogenesis.

Our findings at two time points after CCAO are consistent with the model that dormant neural stem cells initially present in the CA2/CA3 region start expressing Reck as they start proliferating and then migrate into other areas of the hippocampus. Our findings, however, are also consistent with other models: for example, Reck expression is induced independently in many areas with differential time courses. The relationship between Reck expression, cell proliferation, and migration need to be clarified in future studies, for instance, using live imaging green fluorescent protein-tagged cells. Nevertheless, Reck may serve as a molecular marker useful in studying biology of brain ischemia and adult neurogenesis.

What would be the role(s) of Reck in these brain cells? Several models can be proposed. First, given the molecular nature of Reck as a membrane-anchored MMP-regulator (Takahashi *et al.* 1998; Oh *et al.* 2001; Miki *et al.* 2007; Omura *et al.* 2009), protection of peri-cellular ECM is an obvious possibility. As the roles of MMPs in tissue damage after ischemia have been documented (Yong *et al.* 2001), the augmented infarction found in the *Reck+/–* mice after a severe form of ischemia (MCAO) can be explained by MMP de-regulation. In this case, Reck may be induced as a part of the intrinsic defense mechanism against tissue damage, although the basally expressed Reck (see UT in Fig. 1b and c) should also play an important role. A recent paper reported that hypoxic pre-treatment before ischemia has neuro-protective effects (Feng *et al.* 2010). Reck may play a role in such pre-conditioning. Our previous studies indicate that Reck expression is affected by various external conditions, including cell density, serum concentration (Hatta *et al.* 2009), growth factor signaling (Sasahara *et al.* 1999), and oxygen concentration (Loayza-Puch *et al.* 2010). Hypoxia down-regulates Reck through microRNAs in human fibrosarcoma cells (Loayza-Puch *et al.* 2010), while limited supply of

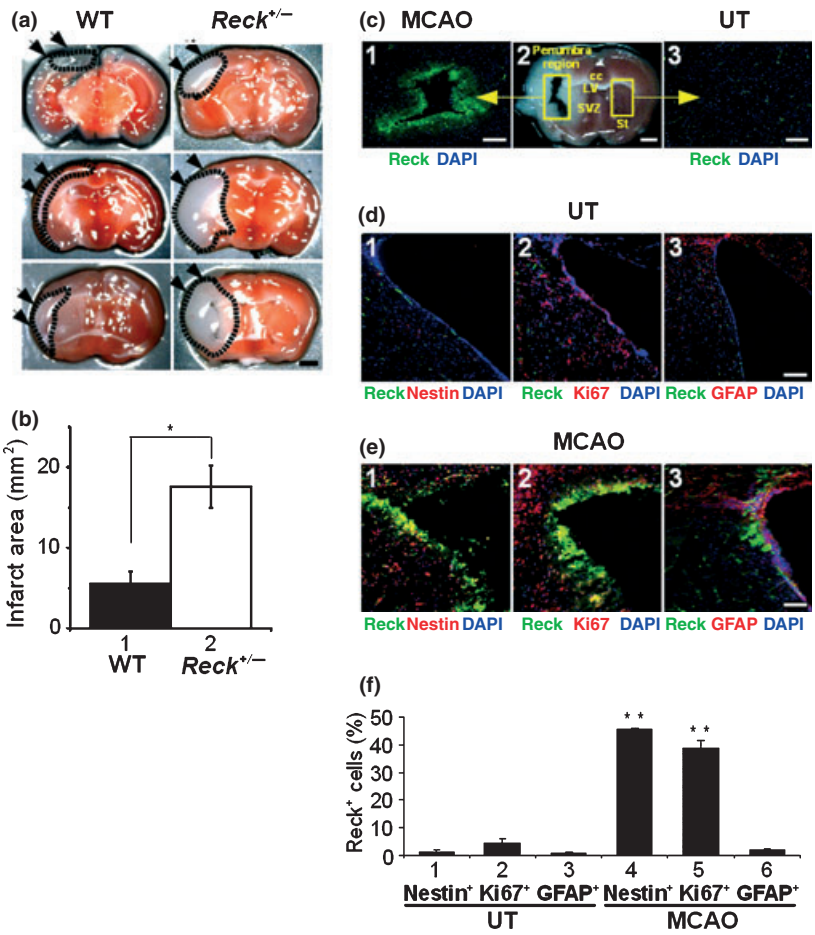

Fig. 8 Reck supports neuroprotection and neurogenesis after MCAO. (a) Three consecutive coronal brain sections (1-mm thick) from *WT* or *Reck+/–* mice at 24 h after MCAO were stained with TTC. Note the larger infarct lesions (white areas) in *Reck+/–* mice (arrowheads). Scale bar: 1 mm. (b) The area of infarction was determined from slice images as shown in (a). Bar represents mean ± SEM ($n = 16$ sections from four animals). (c) *Reck*-immunoreactivity in the penumbla regions (panel 1). Representative slice of TTC staining (panel 2). *Reck*-immunoreactivity in the striatum of UT mice (panel 3). Scale bar: 100 μm (panels 1, 3), 1 mm (panel 2). (d–e) Double staining of Reck and Nestin (panel 1), Ki67 (panel 2) and GFAP (panel 3) cells in subventricular zone of the striatum. Scale bar: 100 μm. (f) Quantification of Reck immunoreactivity among Nestin (bars 1, 4), Ki67 (bars 2, 5) and GFAP (bars 3, 6) positive cells. Bar represents mean ± SEM ($n = 40$–50 slices from four animals). $^{**}p < 0.01$ vs. UT (Student's *t*-test). $^{*}p < 0.05$.

serum up-regulates Reck in mouse embryo fibroblasts (Hatta *et al.* 2009). *Reck* expression may be triggered by a net effect of changes in several external conditions induced by ischemia.

Second, Reck expression may be induced as a part of the de-differentiation program operating to protect ECM niche and/or to resume self-renewal. In fact, in developing CNS, Reck is known to reinforce Notch-signaling by protecting Notch-ligands from proteolytic shedding, leading to the suppression of neuronal differentiation and the production of sufficient number of NPCs (Muraguchi *et al.* 2007). Third, as MMPs are known to play beneficial roles in mildly damaged tissues by promoting tissue repair (Yong *et al.* 2001), the ischemia-induced Reck (a protector of ECM) may serve as a counteracting regulator for MMPs (destroyers of ECM) in the integral ECM-remodeling machinery. Forth, it has been demonstrated in fibroblasts that Reck stabilizes focal adhesions, anterior–posterior polarity, and direction in migration (Morioka *et al.* 2009). Reck may therefore be important for adhesion, cell polarity, and migration of NPCs as well. Finally, it is feasible that Reck is important for process extension and axonal guidance, as these events largely depend on ECM components and cell surface molecules (Ellison *et al.* 1999; Lukes *et al.* 1999; Sykova and Vargova 2008). These models may not be mutually exclusive and warrant further investigations.

In *Reck+/–* mice, the ability of hippocampal slices to exhibit fEPSP was restored by day 7 after CCAO, but LTP remained undetectable (Fig. 4). We found the enhancement of NR2C subunit of NMDAR (Fig. 5). NR2C up-regulation in *Reck+/–* mice does not seem to be affected to LTP induction (Hrabetova *et al.* 2000), but glutamate excitotoxicity (Small *et al.* 1997; Kadotani *et al.* 1998). The transient loss of fEPSP (and LTP) after CCAO, which was also seen in *WT* mice (Fig. 4d), may be attributable to the changes in micro-environment as previously suggested (Reeves *et al.* 2003): for example, excessive degradation of ECM components or cell surface molecules such as laminin (Chen and Strickland 1997; Nakagami *et al.* 2000) and integrin-associated proteins (Chang *et al.* 2001). In fact, previous studies indicate that hippocampal slices treated with plasmin failed to maintain LTP due mainly to the loss of laminin (Nakagami *et al.* 2000) and that mice lacking dystroglycan, a membrane receptor for laminin/basement membrane, failed to show hippocampal LTP (Moore *et al.* 2002). Significantly reduced

laminin-immunoreactivity in *Reck*+/− mice (Fig. 6b) may therefore underlie the loss of LTP at day 7 after ischemia. Our immunohistochemical data suggest that laminin is most abundant in vascular basement membrane (Fig. 6c). In fact, Reck is essential for vascular remodeling during embryogenesis (Oh *et al.* 2001) as well as in adult animals (Chandana *et al.*, unpublished). Whether LTP is affected by reduced laminin (or some other components, for example, glutamate receptor subunit imbalance) associated with neurons or due indirectly to vascular damage is an important issue to be clarified in future studies.

Our study has demonstrated the ability of Reck to reduce tissue damage after severe ischemia and to support the recovery of neural plasticity after mild ischemia. Given this molecular marker/effector, it will be interesting to study the correlation between the level of Reck expression and the consequences of a stroke or other forms of ischemic brain damages among patients. It will also be interesting to test whether drugs up-regulating Reck are able to reduce tissue damage and/or to promote functional recovery after cerebral ischemia in animal models.

Acknowledgements

We are grateful to Yasuhiro Maeda, Mamiko Hatta, Kanako Yuki, Takao Miki, Junji Itou, Tomoko Matsuzaki, and Yoko Yoshida for their help and technical advices in various aspects of this study, Youshi Fujita for advising on ischemia operation, Aiko Nishimoto and Hai-Ou Gu for laboratory managements, and Aki Miyazaki for secretarial assistance. We also thank Dr. Richard Bergeron for his critical reading of the manuscript. This work was supported by grants from Grant-in-Aid for Scientific Research on Priority Areas-Molecular Brain Science-from the Ministry of Education, Culture, Sports, Science and Technology of Japan.

Competing interest statement

The authors declare no competing financial interests.

Supporting information

Additional Supporting Information may be found in the online version of this article:

Figure S1. Reck affects neural precursor expression.

As a service to our authors and readers, this journal provides supporting information supplied by the authors. Such materials are peer-reviewed and may be re-organized for online delivery, but are not copy-edited or typeset. Technical support issues arising from supporting information (other than missing files) should be addressed to the authors.

References

Bickler P. E., Fahlman C. S. and Taylor D. M. (2003) Oxygen sensitivity of NMDA receptors: relationship to NR2 subunit composition and hypoxia tolerance of neonatal neurons. *Neuroscience* **118**, 25–35.

Bliss T. V. and Collingridge G. L. (1993) A synaptic model of memory: long-term potentiation in the hippocampus. *Nature* **361**, 31–39.

Calabresi P., Marfia G. A., Centonze D. *et al.* (1999) Sodium influx plays a major role in the membrane depolarization induced by oxygen and glucose deprivation in rat striatal spiny neurons. *Stroke* **30**, 171–179.

Calabresi P., Centonze D. and Bernardi G. (2000) Cellular factors controlling neuronal vulnerability in the brain: a lesson from the striatum. *Neurology* **55**, 1249–1255.

Calabresi P., Centonze D., Pisani A. *et al.* (2003) Synaptic plasticity in the ischaemic brain. *Lancet Neurol.* **2**, 622–629.

Centonze D., Marfia G. A., Pisani A. *et al.* (2001) Ionic mechanisms underlying differential vulnerability to ischemia in striatal neurons. *Prog. Neurobiol.* **63**, 687–696.

Chang H. P., Ma Y. L., Wan F. J. *et al.* (2001) Functional blocking of integrin-associated protein impairs memory retention and decreases glutamate release from the hippocampus. *Neuroscience* **102**, 289–296.

Chen Z. L. and Strickland S. (1997) Neuronal death in the hippocampus is promoted by plasmin-catalyzed degradation of laminin. *Cell* **91**, 917–925.

Crepel V., Hammond C., Krnjevic K. *et al.* (1993) Anoxia-induced LTP of isolated NMDA receptor-mediated synaptic responses. *J. Neurophysiol.* **69**, 1774–1778.

Dirnagl U., Simon R. P. and Hallenbeck J. M. (2003) Ischemic tolerance and endogenous neuroprotection. *Trends Neurosci.* **26**, 248–254.

Ellison J. A., Barone F. C. and Feuerstein G. Z. (1999) Matrix remodeling after stroke. De novo expression of matrix proteins and integrin receptors. *Ann. N Y Acad. Sci.* **890**, 204–222.

Ernst C. and Christie B. R. (2005) Nestin-expressing cells and their relationship to mitotically active cells in the subventricular zones of the adult rat. *Eur. J. Neurosci.* **22**, 3059–3066.

Ethell I. M. and Ethell D. W. (2007) Matrix metalloproteinases in brain development and remodeling: synaptic functions and targets. *J. Neurosci. Res.* **85**, 2813–2823.

Felling R. J., Snyder M. J., Romanko M. J. *et al.* (2006) Neural stem/progenitor cells participate in the regenerative response to perinatal hypoxia/ischemia. *J. Neurosci.* **26**, 4359–4369.

Feng Y., Rhodes P. G. and Bhatt A. J. (2010) Hypoxic preconditioning provides neuroprotection and increases vascular endothelial growth factor A, preserves the phosphorylation of Akt-Ser-473 and diminishes the increase in caspase-3 activity in neonatal rat hypoxic-ischemic model. *Brain Res.* **1325**, 1–9.

Fujimoto M., Takagi Y. and Aoki T. *et al.* (2008) Tissue inhibitor of metalloproteinases protect blood-brain barrier disruption in focal cerebral ischemia. *J. Cereb. Blood Flow Metab.* **28**, 1674–1685.

Gidday J. M. (2006) Cerebral preconditioning and ischaemic tolerance. *Nat. Rev. Neurosci.* **7**, 437–448.

Gillardon F., Kiprianova I. and Sandkuhler J. *et al.* (1999) Inhibition of caspases prevents cell death of hippocampal CA1 neurons, but not impairment of hippocampal long-term potentiation following global ischemia. *Neuroscience* **93**, 1219–1222.

Gu Z., Kaul M., Yan B. *et al.* (2002) S-nitrosylation of matrix metalloproteinases: signaling pathway to neuronal cell death. *Science* **297**, 1186–1190.

Hammond C., Crepel V. and Gozlan H. *et al.* (1994) Anoxic LTP sheds light on the multiple facets of NMDA receptors. *Trends Neurosci.* **17**, 497–503.

Hatta M., Matsuzaki T. and Morioka Y. *et al.* (2009) Density- and serum-dependent regulation of the Reck tumor suppressor in mouse embryo fibroblasts. *Cell. Signal.* **21**, 1885–1893.

Hrabetova S., Serrano P., Blace N. *et al.* (2000) Distinct NMDA receptor subpopulations contribute to long-term potentiation and long-term depression induction. *J. Neurosci.* **20**, RC81.

Ihara M., Tomimoto H. and Kinoshita M. *et al.* (2001) Chronic cerebral hypoperfusion induces MMP-2 but not MMP-9 expression in the microglia and vascular endothelium of white matter. *J. Cereb. Blood Flow Metab.* **21**, 828–834.

Imamura Y., Matsumoto N., Kondo S. *et al.* (2003) Possible involvement of Rap1 and Ras in glutamatergic synaptic transmission. *Neuroreport* **14**, 1203–1207.

Imamura Y., Ma C. L. and Pabba M. *et al.* (2008) Sustained saturating level of glycine induces changes in NR2B-containing-NMDA receptor localization in the CA1 region of the hippocampus. *J. Neurochem.* **105**, 2454–2465.

Kadotani H., Namura S. and Katsuura G. *et al.* (1998) Attenuation of focal cerebral infarct in mice lacking NMDA receptor subunit NR2C. *Neuroreport* **9**, 471–475.

Kawashima S., Imamura Y. and Chandana E. P. *et al.* (2008) Localization of the membrane-anchored MMP-regulator RECK at the neuromuscular junctions. *J. Neurochem.* **104**, 376–385.

Kimura T., Okada A., Yatabe T. *et al.* (2010) RECK is up-regulated and involved in chondrocyte cloning in human osteoarthritic cartilage. *Am. J. Pathol.* **176**, 2858–2867.

Koizumi S., Shigemoto-Mogami Y. and Nasu-Tada K. *et al.* (2007) UDP acting at P2Y6 receptors is a mediator of microglial phagocytosis. *Nature* **446**, 1091–1095.

van Lent P. L., Span P. N. and Sloetjes A. W. *et al.* (2005) Expression and localisation of the new metalloproteinase inhibitor RECK (reversion inducing cysteine-rich protein with Kazal motifs) in inflamed synovial membranes of patients with rheumatoid arthritis. *Ann. Rheum. Dis.* **64**, 368–374.

Li L., Lundkvist A. and Andersson D. *et al.* (2008) Protective role of reactive astrocytes in brain ischemia. *J. Cereb. Blood Flow Metab.* **28**, 468–481.

Lin T. N., He Y. Y. and Wu G. *et al.* (1993) Effect of brain edema on infarct volume in a focal cerebral ischemia model in rats. *Stroke* **24**, 117–121.

Lo E. H., Dalkara T. and Moskowitz M. A. (2003) Mechanisms, challenges and opportunities in stroke. *Nat. Rev. Neurosci.* **4**, 399–415.

Loayza-Puch F., Yoshida Y., Matsuzaki T. *et al.* (2010) Hypoxia and RAS-signaling pathways converge on, and cooperatively downregulate, the RECK tumor-suppressor protein through microRNAs. *Oncogene* **29**, 2638–2648.

Lukes A., Mun-Bryce S. and Lukes M. *et al.* (1999) Extracellular matrix degradation by metalloproteinases and central nervous system diseases. *Mol. Neurobiol.* **19**, 267–284.

Mash D. C., Ffrench-Mullen J. and Adi N. *et al.* (2007) Gene expression in human hippocampus from cocaine abusers identifies genes which regulate extracellular matrix remodeling. *PLoS ONE* **2**, e1187.

Meighan S. E., Meighan P. C., Choudhury P. *et al.* (2006) Effects of extracellular matrix-degrading proteases matrix metalloproteinases 3 and 9 on spatial learning and synaptic plasticity. *J. Neurochem.* **96**, 1227–1241.

Miki T., Takegami Y., Okawa K. *et al.* (2007) The reversion-inducing cysteine-rich protein with Kazal motifs (RECK) interacts with membrane type 1 matrix metalloproteinase and CD13/aminopeptidase N and modulates their endocytic pathways. *J. Biol. Chem.* **282**, 12341–12352.

Moore S. A., Saito F. and Chen J. *et al.* (2002) Deletion of brain dystroglycan recapitulates aspects of congenital muscular dystrophy. *Nature* **418**, 422–425.

Morioka Y., Monypenny J., Matsuzaki T. *et al.* (2009) The membrane-anchored metalloproteinase regulator RECK stabilizes focal adhesions and anterior-posterior polarity in fibroblasts. *Oncogene* **28**, 1454–1464.

Muraguchi T., Takegami Y. and Ohtsuka T. *et al.* (2007) RECK modulates Notch signaling during cortical neurogenesis by regulating ADAM10 activity. *Nat. Neurosci.* **10**, 838–845.

Nagy V., Bozdagi O., Matynia A. *et al.* (2006) Matrix metalloproteinase-9 is required for hippocampal late-phase long-term potentiation and memory. *J. Neurosci.* **26**, 1923–1934.

Nakagami Y., Abe K. and Nishiyama N. *et al.* (2000) Laminin degradation by plasmin regulates long-term potentiation. *J. Neurosci.* **20**, 2003–2010.

Nakaji K., Ihara M. and Takahashi C. *et al.* (2006) Matrix metalloproteinase-2 plays a critical role in the pathogenesis of white matter lesions after chronic cerebral hypoperfusion in rodents. *Stroke* **37**, 2816–2823.

Nakatomi H., Kuriu T. and Okabe S. *et al.* (2002) Regeneration of hippocampal pyramidal neurons after ischemic brain injury by recruitment of endogenous neural progenitors. *Cell* **110**, 429–441.

Namba T., Mochizuki H., Onodera M. *et al.* (2005) The fate of neural progenitor cells expressing astrocytic and radial glial markers in the postnatal rat dentate gyrus. *Eur. J. Neurosci.* **22**, 1928–1941.

Nishimura M., Izumiya Y. and Higuchi A. *et al.* (2008) Adiponectin prevents cerebral ischemic injury through endothelial nitric oxide synthase dependent mechanisms. *Circulation* **117**, 216–223.

Noda M. and Takahashi C. (2007) Recklessness as a hallmark of aggressive cancer. *Cancer Sci.* **98**, 1659–1665.

Noda M., Oh J., Takahashi R. *et al.* (2003) RECK: a novel suppressor of malignancy linking oncogenic signaling to extracellular matrix remodeling. *Cancer Metastasis Rev.* **22**, 167–175.

Oh J., Takahashi R., Kondo S. *et al.* (2001) The membrane-anchored MMP inhibitor RECK is a key regulator of extracellular matrix integrity and angiogenesis. *Cell* **107**, 789–800.

Omura A., Matsuzaki T. and Mio K. *et al.* (2009) RECK Forms Cowbell-shaped Dimers and Inhibits Matrix Metalloproteinase-catalyzed Cleavage of Fibronectin. *J. Biol. Chem.* **284**, 3461–3469.

Pforte C., Henrich-Noack P. and Baldauf K. *et al.* (2005) Increase in proliferation and gliogenesis but decrease of early neurogenesis in the rat forebrain shortly after transient global ischemia. *Neuroscience* **136**, 1133–1146.

Reeves T. M., Prins M. L. and Zhu J. *et al.* (2003) Matrix metalloproteinase inhibition alters functional and structural correlates of deafferentation-induced sprouting in the dentate gyrus. *J. Neurosci.* **23**, 10182–10189.

Rosell A., Ortega-Aznar A., Alvarez-Sabin J. *et al.* (2006) Increased brain expression of matrix metalloproteinase-9 after ischemic and hemorrhagic human stroke. *Stroke* **37**, 1399–1406.

Sasahara R. M., Takahashi C. and Noda M. (1999) Involvement of the Sp1 site in ras-mediated downregulation of the RECK metastasis suppressor gene. *Biochem. Biophys. Res. Commun.* **264**, 668–675.

Small D. L., Poulter M. O. and Buchan A. M. *et al.* (1997) Alteration in NMDA receptor subunit mRNA expression in vulnerable and resistant regions of in vitro ischemic rat hippocampal slices. *Neurosci. Lett.* **232**, 87–90.

Sternlicht M. D. and Werb Z. (2001) How matrix metalloproteinases regulate cell behavior. *Annu. Rev. Cell Dev. Biol.* **17**, 463–516.

Stoppini L., Buchs P. A. and Muller D. (1991) A simple method for organotypic cultures of nervous tissue. *J. Neurosci. Methods* **37**, 173–182.

Sykova E. and Vargova L. (2008) Extrasynaptic transmission and the diffusion parameters of the extracellular space. *Neurochem. Int.* **52**, 5–13.

Takahashi C., Sheng Z., Horan T. P. *et al.* (1998) Regulation of matrix metalloproteinase-9 and inhibition of tumor invasion by the

membrane-anchored glycoprotein RECK. *Proc. Natl Acad. Sci. USA* **95**, 13221–13226.

Tsuji K., Aoki T., Tejima E. *et al.* (2005) Tissue plasminogen activator promotes matrix metalloproteinase-9 upregulation after focal cerebral ischemia. *Stroke* **36**, 1954–1959.

Wang Y. F., Tsirka S. E. and Strickland S. *et al.* (1998) Tissue plasminogen activator (tPA) increases neuronal damage after focal cerebral ischemia in wild-type and tPA-deficient mice. *Nat. Med.* **4**, 228–231.

Wang L., Zhang Z. G., Zhang R. L. *et al.* (2006) Matrix metalloproteinase 2 (MMP2) and MMP9 secreted by erythropoietin-activated endothelial cells promote neural progenitor cell migration. *J. Neurosci.* **26**, 5996–6003.

Whitlock J. R., Heynen A. J. and Shuler M. G. *et al.* (2006) Learning induces long-term potentiation in the hippocampus. *Science* **313**, 1093–1097.

Yang G., Kitagawa K., Matsushita K. *et al.* (1997) C57BL/6 strain is most susceptible to cerebral ischemia following bilateral common carotid occlusion among seven mouse strains: selective neuronal death in the murine transient forebrain ischemia. *Brain Res.* **752**, 209–218.

Yong V. W., Power C., Forsyth P. *et al.* (2001) Metalloproteinases in biology and pathology of the nervous system. *Nat. Rev. Neurosci.* **2**, 502–511.

Zhao B. Q., Wang S., Kim H. Y. *et al.* (2006) Role of matrix metalloproteinases in delayed cortical responses after stroke. *Nat. Med.* **12**, 441–445.

